Colloids and Surfaces B: Biointerfaces 104 (2013) 289–293

Contents lists available at SciVerse ScienceDirect

Colloids and Surfaces B: Biointerfaces

journal homepage: www.elsevier.com/locate/colsurfb

Combined atomic force microscopy and spectroscopic ellipsometry applied to the analysis of lipid–protein thin films

Eric Finot[a,*], Laurent Markey[a], Francis Hane[b], Mathias Amrein[c], Zoya Leonenko[b,d]

[a] Laboratoire Interdisciplinaire Carnot de Bourgogne, UMR 6303 CNRS, Universit'e de Bourgogne, 9 Avenue A. Savary, F-21078, Dijon, France
[b] Department of Biology, University of Waterloo, N2L 3G1, ON, Canada
[c] Department of Cell Biology and Anatomy, Faculty of Medicine, University of Calgary, T2N 4N1, AB, Canada
[d] Department of Physics and Astronomy, University of Waterloo, N2L 3G1, ON, Canada

ARTICLE INFO

Article history:
Received 30 July 2012
Received in revised form
11 November 2012
Accepted 15 December 2012
Available online 25 December 2012

Keywords:
Phospholipids
Pulmonary surfactant
BLES
Langmuir–Blodgett monolayer
ITO
Ellipsometry
Atomic force microscopy

ABSTRACT

Pulmonary surfactant is a complex mixture of phospholipids and proteins and forms a thin film at the lung alveolar interface separating air from liquid environment. The film reduces the work of breathing during repeatable compressions of the alveoli which form a characteristic multilayer upon compression. In this work, we investigated the structure of bovine lipid extract surfactant (BLES). We analysed the BLES films by atomic force microscopy (AFM) and spectroscopic ellipsometry (SE) in order to provide combined characterization of both morphology and thickness of surfactant films. We show how the spectroscopic ellipsometry can be used to supplement the data obtained by AFM. We demonstrate that indium tin oxide (ITO) substrate used for spectroscopic ellipsometry is preferable over glass substrate to enhance the optical contrast. An optical model was proposed to account for non-uniform film morphology. We obtained good correlations between the multilayer surface coverage, determined by both AFM and SE. SE measures the thickness of the first uniform monolayer as 2.6 nm that cannot be achieved by AFM imaging alone.

1. Introduction

Pulmonary surfactant (PS) forms a thin molecular film that covers the lung epithelium and helps to reduce the work of breathing by reducing the surface tension of the interface to near-zero values. PS is composed of a mixture of phospholipids (90%) and surfactant specific proteins (10%) and is essential for normal respiration and the structural stability of the lung. The lack or malfunction of the surfactant leads to neonatal respiratory distress syndrome (NRDS) [1,2] in premature infants or acute respiratory distress syndrome (ARDS) in adults. The treatment involves administration of surfactant replacement formulations such as Bovine Lipid Extract Surfactant (BLES) by endotracheal tube. In order to create better surfactant formulations, it is important to understand in detail the surfactant structure and function [3].

Atomic force microscopy (AFM) is widely used to study lipid films and has been applied previously to study structural organization of pulmonary surfactant (for example [4–6]). Von Nahmen et al. [7] showed that functional surfactant forms a characteristic pattern of multilayers upon compression. This multilayer structure is a characteristic property of functional surfactant and is affected by the presence of cholesterol [4,5,8].

In order to study the morphology of BLES films using AFM the film needs to be deposited onto a solid substrate. Supported lipid membranes and monolayers in general are an important aspect of modern bio-nano-technology research, and have been investigated by various instrumental methods [9]. Combinations of ellipsometry and quartz crystal microbalance as well as ellipsometry and X-ray diffraction were reported in Refs. [10] and [11]. In previous publications, lipid films were studied deposited on a variety of substrates, such as mica [12], gold [13], glass, [14] and polystyrene surfaces [15].

Although pulmonary surfactant has been studied using ellipsometry [16,17], our work ([18] and present work) is the first study where ellipsometry is used in combination with the atomic force microscopy (AFM), which accounts for the complex multilayer structure of BLES and provides more detailed information on the structure of these films.

AFM is a high resolution imaging technique which provides a nm scale lateral resolution and 0.1 nm resolution in height. Although AFM is an extremely useful method for imaging lipid monolayers and membranes, one cannot measure the thickness of the inform surfactant layer, which is assumed to be a monolayer underneath the multilayers, without indenting through the film.

* Corresponding author.
E-mail address: Eric.Finot@u-bourgogne.fr (E. Finot).

0927-7765/$ – see front matter © 2012 Elsevier B.V. All rights reserved.
http://dx.doi.org/10.1016/j.colsurfb.2012.12.013

We used spectroscopic ellipsometry in addition to AFM to determine the thickness of the monolayer and to resolve the multilayer organization.

Ellipsometry is a highly sensitive optical technique used to determine the thickness of thin films at solid/air or liquid/air interfaces. This technique is based on measuring the changes in the ellipsometric angles, ψ and Δ, when elliptically polarized light is reflected off a planar surface, and thus the mass of adsorbed material can be deduced via thorough mathematical analysis of ellipsometric angles [19]. Although the mass resolution of ellipsometry is high, about 5–10 ng/cm^2 [19], the analysis of ellipsometric angles is complicated, as ψ and Δ are a function of both the thickness of the film and the refractive index of the material. In order to overcome this difficulty, a modification of the standard ellipsometric device has been made, which is referred to as spectroscopic ellipsometry [20]. The major advantage of spectroscopic ellipsometry over other measurement techniques is the precision of thickness measurements. Using, ellipsometry, one is able to resolve optical parameters as a function of time, which makes it advantageous for probing dynamic systems. Ellipsometry has been used extensively to study peptide and lipid assemblies. Benes et al. [21] used ellipsometry to show the formation of supported bilayers on mica followed by their degradation when exposed to phospholipase *A*2 by a mechanism that involved a decrease in layer density while layer thickness remained constant. Hernendez et al. used ellipsometry to study the effect of the serum protein fibrinogen concentration on surface activity at the air/water interface on films of DPPC lipids [22]. Research by Malmsten et al. [23] used ellipsometry to study amyloid-β deposits by measuring the Ca^{2+} induced adsorption of the lipoprotein with bound amyloid-β peptide to the modified mica slides. Mica is commonly used to study thin bioorganic films by AFM but in case of ellipsometry only qualitative measurements of simple adsorption can be achieved with mica. More complex layered films cannot be analysed on mica because mica has a pronounced layered structure itself. In order to obtain more detailed information on complex layered structure of BLES film and its thickness we supported surfactant film on glass and indium tin oxide (ITO) substrates.

A combination of AFM and ellipsometry is not a common approach to study supported lipid films. A first attempt has been made recently by Vidawati et al. [24] where mean lipid film thickness was estimated by ellipsometry. In the present work we used AFM and spectroscopic ellipsometry to resolve a complex multilayer structure and showed a good correlation of multilayer thicknesses, determined by both AFM and the spectroscopic ellipsometry. The thickness of the first uniform monolayer, which was not accessible by AFM, was measured by ellipsometry only.

2. Materials and methods

We used bovine lipid extract surfactant (BLES), which is a hydrophobic extract of bovine lung lavage that differs from natural surfactant in the lack of surfactant specific proteins *SP-A* and *SP-D* and cholesterol. Phosphatidylcholines (PC) represent 80% of its mass with half of the PC being the saturated dipalmitoylphosphatidylcholine (DPPC).

Supported BLES films were prepared using Langmuir–Blodgett technique which is commonly used to deposit thin films onto solid substrates [25]. BLES films were deposited on glass or ITO substrates at a constant compression of 45 mN/m.

We modified the substrate by depositing a thin layer of ITO (Sn-doped In_2O_3) to optically enhance the contrast with the lipid film. Common in photovoltaic devices, heat reflecting mirrors and other optoelectronic applications, ITO is one of the most intensively studied transparent conductive oxide materials. Its high optical transparency, good electrical conductivity, excellent substrate adherence, high thermal stability and chemical inertness make ITO an excellent candidate for a substrate to deposit lipid films.

The ITO substrates were prepared by sputtering. The soda lime glass substrates with a size of 50 mm × 50 mm and a thickness of 1 mm were cleaned using ultrasound in acetone and pure water and then blow-dried with air. It was then placed under vacuum at 10^3 Pa to a holder at a negative bias voltage of 200 V in a close proximity of the target made of In–Sn alloy (10 wt%). The working pressure of the process gas O_2 was set to 0.5 bar. The gas is ionized with an arc current fixed at 20 A. A film of ITO of 60 nm thick and resistance of 20 Ω was deposited in 5 min.

Supported BLES films were imaged in air using NanoWizard AFM (JPK Instruments, AG) in intermittent contact mode. From AFM imaging, we deduced the height distribution through cross-section analysis and produced a height histogram. The effective thickness of the patches was then obtained by analyzing the surface area of the peaks on the histogram. Spectroscopic ellipsometric measurements were carried out using a phase modulated ellipsometer (UVISEL, Jobin Yvon) in the wavelength range between 250 and 800 nm at a 65° light reflection angle.

Ellipsometry is an indirect technique where the signals issued from the measurements are the rotation angles ψ and Δ defined by the ratio ρ of the complex reflection coefficient R_p and R_s for light polarized parallel (p) and perpendicular (s) respectively to the plane of incidence:

$$\rho = \frac{R_p}{R_s} = tan\psi \exp^{i\Delta} \quad (1)$$

If the sample is composed of multilayers of thin films, each layer contributes in the variation of ψ and Δ. The values of the thickness t and the refractive index n and the extinction coefficient k were evaluated by fitting the experimental angles ψ and Δ to Fresnel equations using a least-square algorithm. The analysis of spectroscopic ellipsometry data was carried out using two models, which employ regression analysis. In a first approach (Model 1) similar to Ref. [24], the BLES film was modelled by a thin layer with uniform complete coverage. Two parameters were determined using this model: refractive index n and effective thickness t. We applied the same procedure described by Arwin and Aspnes [26]. The effective medium approximations provide the means to determine optical constants but also the morphology of the materials that constitute the film layer. We have used the Bruggeman EMA (sometimes referred to as the coherent potential approximation) which does not assume a mean film thickness, but rather weights of constituent materials according to their volume fractions and dielectric functions [27]. More complex Model 2 considers 6 output parameters: the height of the first monolayer at the ITO interface with complete coverage and the coverage fraction of the four upper bilayer stacks (Fig. 2A). The refractive index n of the BLES was assumed constant in all layers. The thickness of patches of each layer determined from the analysis of AFM images was used as the input parameter.

3. Results and discussion

AFM was used to characterize the architecture of the BLES film. Fig. 1 shows the multilayered structure of BLES film, demonstrating that the surface coverage is not uniform in each layer, but reveals patches of lateral dimensions varying between 0.1 μm^2 and 1 μm^2 in area. The overall height of bilayer stacks measured by AFM is approximately the same, 20 nm for glass and ITO substrates. The single bilayer patches have thickness around 5 nm on both glass or ITO substrate. The surface coverage of each layer of patches measured by AFM is shown in Fig. 2 by the red bar for both the glass and ITO substrate. However, the surface coverage of the patches varies

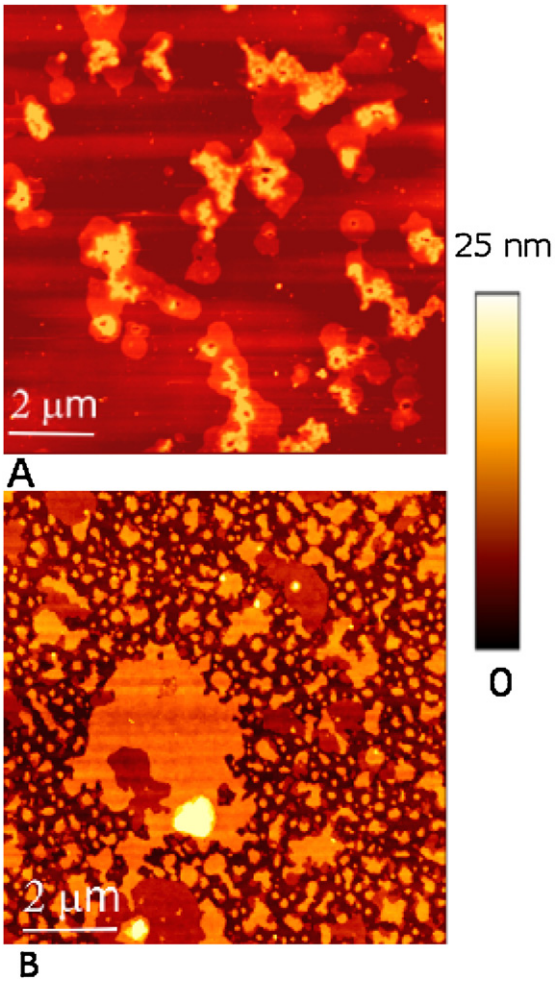

Fig. 1. AFM topography images showing BLES films supported: (A) onto glass, (B) onto ITO substrate.

from one type of substrate to another. The ITO substrate, is a negatively charged surface, and appears to develop a more extended patch coverage compared to glass substrate. The second bilayer (light brown color, Fig. 2B) on ITO covers around 80% of the surface, whereas on glass it covers less than 30% (Fig. 2A). Once the second layer of patches is developed, two or three other layers can

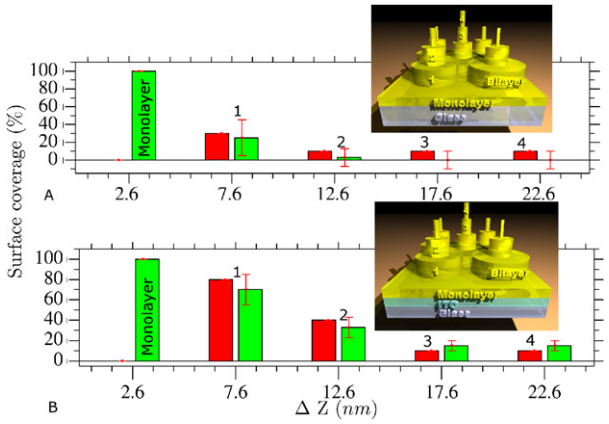

Fig. 2. Surface coverage of BLES stacks determined in red by AFM and in green by ellipsometry using the model 2 (A) on glass, (B) on ITO. The first bar corresponds to the first monolayer, the thickness of which is determined by spectroscopy ellipsometry. The error bars correspond to the margin of tolerance of the model. Schematics in each case shows formation of multilayer stacks on (A) glass and on (B) ITO substrate.

Table 1
Model 1: effective thickness t_{eff} and refractive index n of the BLES film deposited on either glass and ITO substrate.

	t_{eff} (nm)	n
Glass	3.9 ± 0.3	1.5 ± 0.05
ITO	6.8 ± 0.1	1.47 ± 0.02

be formed on top of each other, thus reducing gradually the surface coverage with height.

The background layer (darker color) fully covers the substrate in both cases – ITO and glass (Fig. 1A and B) and corresponds to a monolayer, as determined by force measurements. We measured adhesion forces on BLES film and showed that a much higher adhesion is observed on BLES monolayer, which correlates well with our previously published data [6]. There is no simple way to determine the thickness of the monolayer using AFM cross-section analysis alone.

Once the type of morphology is established, spectroscopic ellipsometry (SE) provides a reasonably accurate method for the determination of optical constants of dielectric thin films. The phase modulation as well as the spectroscopic analysis enable us to determine the thickness and refractive index of the multilayers separately.

Our goal was to confirm the architecture of BLES multilayers by spectroscopic ellipsometry. Ellipsometric spectra were first collected on a glass substrate. Changes in the ellipsometric angles between bare and covered glass substrate were found to be less than 0.5° in ψ (Fig. 3A) in the far UV regime and a shift of 2° in Δ (Fig. 3C). Ellipsometric spectra were then fitted with optical models 1 and 2 to extract physical parameters of BLES structure.

In a first approach (Model 1), the BLES film has been modelled by a monolayer of complete coverage, with unknown effective thickness, t_{eff}, and refractive index n. The BLES film is assumed to be transparent ($k = 0$) with negligible wavelength dependence of n. Parameters t_{eff} and n were determined using Model 1 and are shown in Table 1.

The optical constant, n, that we obtained agrees with the reported data for lipids [28]. The effective thickness of around 3.9 nm is higher than what is expected for a monolayer (~2.5 nm). However, these results are subject to considerable uncertainty due to the simplicity of the model.

To improve this, we applied Model 2 described earlier in Methods and determined the 6 parameters. Index profile was simulated using a stack of several layers, for which the surface coverage was decreasing with height. The first parameter, thickness t_0 corresponding to a first layer with complete coverage, presumably a monolayer (first green bar in Fig. 2A) was estimated to be (2.5 ± 0.5) nm. The second parameter n was found to be (1.49 ± 0.06). The third parameter – surface coverage of the second layer, corresponding to bilayer patches, was estimated as 20% (in Fig. 2B, the second green bar found at the height 7.6 nm which correlates to a height of a monolayer plus bilayer of 5 nm). The following parameters – surface coverages of the upper bilayer stacks with the total height of 12.6, 17.6 and 22.6 nm were estimated close to zero. The optical indices of BLES film and glass were very close (1.49 for BLES and 1.6 for glass) therefore it was difficult to distinguish between the film and glass substrate with high sensitivity. To improve the sensitivity we used ITO substrate, which has a significantly different optical index. Optical indices (n, k) of the bare substrate (Glass and ITO) are shown in Fig. 4 and Table 2.

Thus, the ITO is an ideal substrate to deposit lipid films and to satisfy the requirements for the optical contrast (Fig. 4).

Fig. 3B and D show the variations in the ellipsometric angles ψ and Δ for the BLES film deposited on the ITO substrate. Consistent

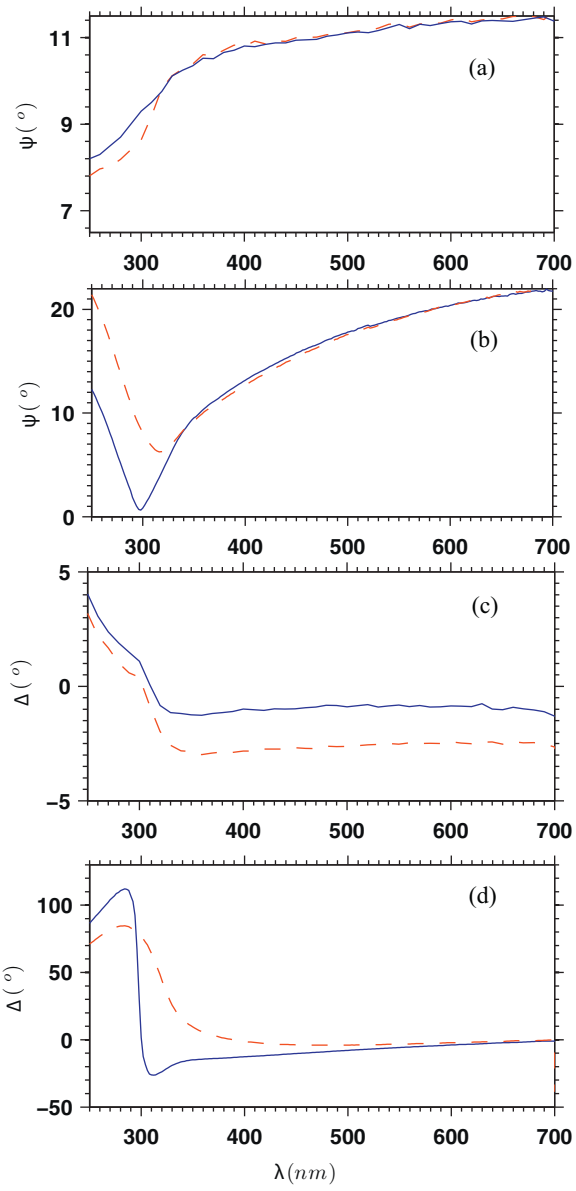

Fig. 3. Spectral changes in ellipsometric angles ψ and Δ for the BLES (blue line) adsorbed onto the bare substrate (red dashed line) in the case of glass (a, c) and ITO (b, d). (For interpretation of the references to color in this figure legend, the reader is referred to the web version of the article.)

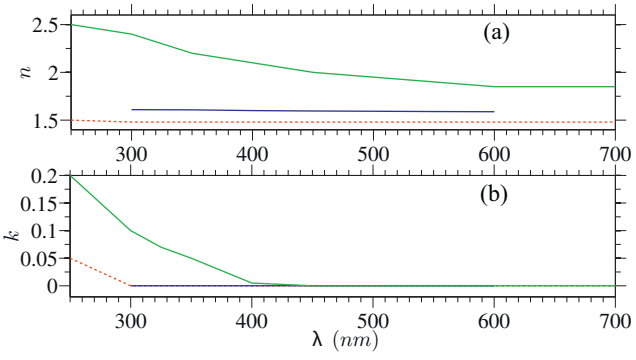

Fig. 4. Spectral variations of the refractive index n and the extinction index k for the ITO layer (in green), the glass substrate (in blue) and the BLES film (in red). (For interpretation of the references to color in this figure legend, the reader is referred to the web version of the article.)

Table 2
Model 2: refractive index n of the BLES film and the surface coverage of the multilayers deposited on either glass and ITO substrate.

	Glass	ITO
1st layer	$n = 1.49$ $t_0 = 2.5$ nm	$n = 1.47$ $t_0 = 2.6$ nm
2nd layer coverage	$(25 \pm 20)\%$	$(1.47 \pm 0.02)\%$
3rd layer coverage	$(2.8 \pm 10)\%$	$(33 \pm 10)\%$
4th layer coverage	$(0 \pm 10)\%$	$(15 \pm 5)\%$
5th layer coverage	$(0 \pm 10)\%$	$(15 \pm 5)\%$

changes in angles of 20° in ψ and more than 100° in Δ were observed in the visible range in all experiments.

In the simplest approach (Model 1), BLES film on ITO was considered as a uniform layer with complete coverage. The effective thickness of the film on ITO was estimated as (6.8 ± 0.1) nm and was larger than on glass (Table 1). This result is consistent with the AFM image analysis, which showed that stacks of BLES film on ITO look larger in surface coverage than that on glass. Note that without AFM imaging, effective thickness larger than ~5–6 nm can be viewed as a bilayer arrangement with complete coverage, leading to a false interpretation. Refractive index n was determined to be 1.47, in agreement to the estimation on glass. The accurate determination of n in the range of (1.4–1.5) was not found to be crucial, as the fit was mostly controlled by the precision of the effective thickness, t_{eff}. Model 2 was applied to the BLES film on ITO substrate similar to the analysis done on glass. BLES film on ITO was considered as composed of five layers: first monolayer with complete coverage and 4 layers of bilayer stacks of 5 nm height each. The results of this analysis are shown in Fig. 2C in green bars. We found that the Model 2 was particularly useful to first confirm the AFM results and to deduce the unknown thickness of the first layer with complete coverage. Error bars on the ellipsometric estimations of the surface coverage are reduced on ITO substrate compared to glass (Fig. 2), which allows for the comparison of the results obtained by AFM and by ellipsometry. The multilayer structures of patches were then optically confirmed on ITO substrate. The ellipsometry does not provide direct information on the distribution and size of the patches, however it allows us to estimate the height of the layer 1, which cannot be determined by AFM alone. From analysis of ellipsometry data using Model 2 we found that the thickness of the first film with complete coverage is 2.6 nm, which corresponds to a thickness of the lipid monolayer consistent with literature data reported for the monolayer thickness [29,30].

4. Conclusion

In conclusion, we showed that spectroscopic ellipsometry in combination with AFM provides a detailed analysis of the BLES surfactant film.

The AFM offers the advantage to determine the morphology of the organization of the film; however, with AFM imaging one can only measure the thickness of the upper discontinuous layers and not the first uniform layer at the interface. On the other hand, it is difficult by using just ellipsometry to determine the type of morphology of the film; but once the number of layers is determined by AFM, the data obtained by ellipsometry can be fit accurately using an optical model and can provide information on the surface coverage of the layers as well as on the unknown thickness of the first monolayer, which has a uniform continuous coverage. This first single monolayer serves as a foundation for the formation of bilayer stacks with various surface coverage.

This combnination of AFM and ellipsometry with novel advanced models can be useful for the characterization of other thin films with complex multilayered morphology. Our future goal is to apply these developemnts to study the early-stage kinetics of

the formation of lipid films using an in situ microfluidics optical setup.

Acknowledgements

The authors acknowledge funding from NSERC (ZL), the Council of Burgundy (EF) and Invited Professorship Award from University of Burgundy, Dijon, to ZL. We are thankful to BLES Biochemicals, London, ON for the donation of BLES for our research.

References

[1] S. Shelley, J. Balis, J. Paciga, C. Espinoza, A. Richman, Biochemical composition of adult human lung surfactant, Lung 160 (1982) 195–206.
[2] R. Veldhuizen, N. Nag, S. Orgeig, F. Possmayer, The role of lipids in pulmonary surfactant, Biochim. Biophys. Acta 1408 (1998) 90–108.
[3] R.H. Notter, Lung Surfactant: Basic Science and Clinical Applications, CRC Press, Boca Raton, FL, 2000.
[4] Z. Leonenko, S. Gill, S. Baoukina, L. Monticelli, J. Doehner, L. Gunasekara, F. Felderer, M. Rodenstein, L.M. Eng, M. Amrein, An elevated level of cholesterol impairs self-assembly of pulmonary surfactant into a functional film, Biophys. J. 93 (2) (2007) 674–683.
[5] L. Gunasekara, S. Schurch, W. Schoel, K. Nag, Z. Leonenko, M. Haufs, M. Amrein, Pulmonary surfactant function is abolished by an elevated proportion of cholesterol, Biochim. Biophys. Acta 1737 (1) (2005) 27–35.
[6] Z. Leonenko, E. Finot, V. Vassiliev, M. Amrein, Effect of cholesterol on the physical properties of pulmonary surfactant films: atomic force measurements study, Ultramicroscopy 106 (8–9) (2006) 687–694.
[7] A. vonNahmen, M. Schenk, M. Sieber, M. Amrein, The structure of a model pulmonary surfactant as revealed by scanning force microscopy, Biophys. J. 72 (1) (1997) 463–469.
[8] E. Finot, Y. Leonenko, B. Moores, L. Eng, M. Amrein, Z. Leonenko, Effect of cholesterol on electrostatics in lipid–protein films of a pulmonary surfactant, Langmuir 26 (3) (2010) 1929–1935.
[9] J.A.I. Gzen, Instrumental methods to characterize molecular phospholipid films on solid supports, Anal. Chem. 17 (2012) 822–838.
[10] I. Carton, L. Malinina, R.P. Richter, Dynamic modulation of the glycosphingolipid content in supported lipid bilayers by glycolipid transfer protein, Biophys. J. 99 (9) (2010) 2947–2956.
[11] P. Seitz, M. Reif, O. Konovalov, R. Jordan, M. Tanaka, Modulation of substrate–membrane interactions by linear poly(2-methyl-2-oxazoline) spacers revealed by X-ray reflectivity and ellipsometry, ChemPhysChem 10 (16) (2009) 2876–2883.
[12] M. Benes, D. Billy, A. Benda, H. Speijer, M. Hof, W. Hermens, Surface-dependent transitions during self-assembly of phospholipid membranes on mica, silica, and glass, Langmuir 20 (23) (2004) 10129–10137.
[13] B.P. Oberts, G.J. Blanchard, Formation of air-stable supported lipid monolayers and bilayers, Langmuir 25 (5) (2009) 2962–2970.
[14] A.P. Shreve, M.C. Howland, A.R. Sapuri-Butti, T.W. Allen, A.N. Parikh, Evidence for leaflet-dependent redistribution of charged molecules in fluid supported phospholipid bilayers, Langmuir 24 (23) (2008) 13250–13253.
[15] O. Santos, T. Arnebrant, Silica supported phospholipid layers doped with GM1: a comparison between different methods, J. Colloid Interface Sci. 329 (2) (2009) 213–221.
[16] N. Bourdos, F. Kollmer, A. Benninghoven, M. Ross, M. Sieber, H. Galla, Analysis of lung surfactant model systems with time-of-flight secondary ion mass spectrometry, Biophys. J. 79 (1) (2000) 357–369.
[17] A. Post, A. Nahmen, M. Schmitt, J. Ruths, H. Riegler, M. Sieber, H. Galla, Pulmonary surfactant protein-c containing lipid films at the air–water interface as a model for the surface of lung alveoli, Mol. Membr. Biol. 12 (1) (1995) 93–99.
[18] Z. Leonenko, M. Amrein, E. Finot, Determination of the molecular architecture of supported lipid–protein films using atomic force microscopy and spectroscopic ellipsometry, J. Microscopy Microanal. 13 (2007) 1588–1589.
[19] R. Richter, A. Brisson, Following the formation of supported lipid bilayers on mica: a study combining AFM, QCM-D, and ellipsometry, Biohys. J. 88 (5) (2005) 3422–3433.
[20] C. Striebel, A. Brecht, G. Gauglitz, Characterization of biomembranes by spectral ellipsometry, surface-plasmon resonance and interferometry with regard to biosensor application, Biosens. Bioelectron. 9 (2) (1994) 139–146.
[21] M. Benes, D. Billy, W. Hermens, M. Hof, Muscovite (mica) allows the characterisation of supported bilayers by ellipsometry and confocal fluorescence correlation spectroscopy, Biol. Chem. 383 (2) (2002) 337–341.
[22] S. Kim, E. Franses, Competitive adsorption of fibrinogen and dipalmitoylphosphatidyleholine at the air/aqueous interface, J. Colloid Interface Sci. 295 (1) (2006) 84–92.
[23] M. Malmsten, U. Kassner, K. Winkler, A. Schmidt, E. Buddecke, R. Saunders, G. Siegel, An ellipsometry-based Alzheimer plaque mimic: effect of beta-amyloid, lipoprotein identity and apolipoprotein E isoform, J. Colloid Interface Sci. 276 (2) (2004) 503–506.
[24] S. Vidawati, J. Sitterberg, U. Bakowsky, U. Rothe, AFM and ellipsometric studies on LB films of natural asymmetric and symmetric bolaamphiphilic archaebacterial tetraether lipids on silicon wafers, Colloids Surf. B-Biointerfaces 78 (2) (2010) 303–309.
[25] L. Netzer, R. Iscovici, J. Sagiv, Adsorbed monolayers versus Langmuir–Blodgett monolayers, why and how? I: from monolayer to multilayer by adsorption, Thin Solid Films 99 (1983) 235–241.
[26] H. Arwin, D. Aspnes, Unambiguous determination of thickness and dielectric function of thin films by spectroscopic ellipsometry, Thin Solid Films 113 (1984) 101–113.
[27] D. Bruggeman, Berechnung verschiedener physikalischer konstanten von heterogenen substanzen, Ann. Phys. (Leipzig) 24 (1935) 636–679.
[28] E. Ross, B. Bondurant, T. Spratt, J. Conboy, D. O'Brien, S. Saavedra, Formation of self-assembled, air-stable lipid bilayer membranes on solid supports, Langmuir 17 (8) (2001) 2305–2307.
[29] M. Thoma, M. Schwendler, H. Baltes, C. Helm, T. Pfohl, H. Riegler, H. Mohwald, Ellipsometry and X-ray reflectivity studies on monolayers of phosphatidylethanolamine and phosphatidylcholine in contact with n-dodecane, n-hexadecane, and bicyclohexyl, Langmuir 12 (7) (1996) 1722–1728.
[30] Q. Huo, S. Russev, T. Hasegawa, J. Nishijo, J. Umemura, G. Puccetti, K. Russell, R. Leblanc, A Langmuir monolayer with a nontraditional molecular architecture, J. Am. Chem. Soc. 122 (33) (2000) 7890–7897.